Journal of Hydroscience and Hydraulic Engineering
Vol. 16, No. 1, May, 1998, 97-108

THREE-DIMENSIONAL FLOW STRUCTURE FOR OVERBANK FLOW IN MEANDERING CHANNELS

By

Yasunori Muto

Ujigawa Hydraulics Laboratory, DPRI
Kyoto University, Fushimi, Kyoto, Japan

Koji Shiono

Department of Civil and Building Engineering
Loughborough University, Loughborough, Leics., UK

Hirotake Imamoto and Taisuke Ishigaki

Ujigawa Hydraulics Laboratory, DPRI
Kyoto University, Fushimi, Kyoto, Japan

SYNOPSIS

Three-dimensional flow structure in meandering channels during flood is discussed based on detailed velocity measurements using a 2 component laser Doppler anemometer. Growth and decay processes of secondary flow in meandering channels and their differences before and after inundation are particularly highlighted. Interaction mechanisms between the lower layer flow (main channel) and the upper layer flow (flood plain) are also of great interest. These topics dealt with in this paper are closely related to the energy loss mechanisms of such flows. The results indicate their relative importance in determining the channel conveyance.

INTRODUCTION

Compound channel flow is known to have a strongly distroted three dimensional nature. Velocity difference between the main channel and the flood plain at the junction region generates this complex nature. The most characteristic flow features, such as strong instant secondary currents and vigorous fluid mixing, can be seen in this region. These internal flow mechanisms generate significant additional flow resistance in the channel hence affecting the channel conveyance (see Fujita (3), Ishigaki (4)). Detailed velocity measurements using a laser Doppler anemometer (LDA) system have recently clarified such internal structures of compound channel flows (Knight & Shiono (7), Tominaga & Nezu (16)). Such data have largely contributed to develop a reliable stage discharge prediction method (e.g. Ackers (1)) and feasible numerical models (e.g. Shiono & Knight (12), Naot et al. (10)).

These studies were mainly focused on a so-called straight compound channel. Thus the accumulated knowledge obtained from this channel may not be applicable to compound meandering channels which have more complicated geometric boundaries (James & Wark (5), Knight & Shiono (8)). Therefore studies on compound meandering channel flow have recently been

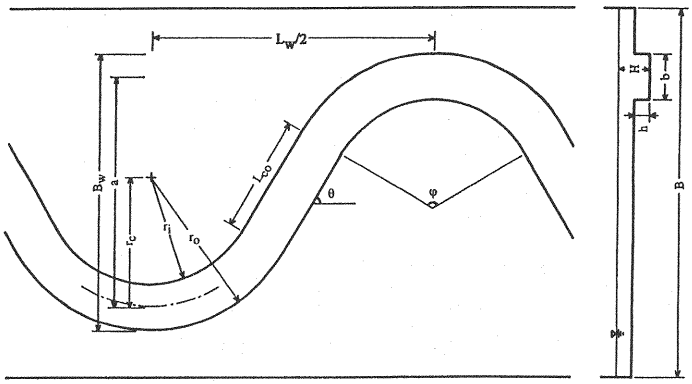

L_W = Meander Wavelength (= Straight Valley Length)
L = Curved Channel Length
L_{co} = Crossover Length
B = Total Width
B_W = Width of Meander Belt
b = Channel Width
a = Double Amplitude
r_c = Bend Central Radius
r_i = Bend Inner Radius
r_o = Bend Outer Radius
H = Water Depth
h = Flood Plain Height
s = Sinuosity (= L/L_W)
φ = Angle of Arc
θ = Angle of Crossover

Fig. 1 Common geometric parameters for meandering channels

Table 1 Geometric parameters for the tested meander channels

Case	Angle of arc φ (°)	Meader Wavelength L_W(mm)	Total width B (mm)	Width of meander B_W (mm)	Bend radius r_c (mm)
R1	60	1502	1200	452	425
R2	120	1848	1200	900	425
R3	180	1700	1200	1000	425

Case	Crossover length L_{CO} (mm)	Crossover angle θ (°)	Sinuosity s	Channel width b (mm)	Flood plain height h (mm)
R1	376	30	1.093	150	53
R2	376	60	1.370	150	53
R3	0	90	1.571	150	53

commenced. A comprehensive research programme using a large scale flume at HR Wallingford, UK, was conducted and the output can be found elsewhere (Sellin et al. (11) and Ervine et al. (2)). Unique features of secondary flow and turbulence in meandering channels with straight and meandering flood plains were also reported by Shiono et al. (13), (14) and (15).

This paper deals with three dimensional structure of the flow in compound meandering channels. Velocity and turbulence data measured in such channels with three different sinuosities (Muto (9)) are analysed. The results not only show new insight into the flow structure, but also give some indications for developing and improving channel design methods.

EXPERIMENTAL SETUP

The experimental flume was made of perspex with a rectangular cross section whose dimensions were 10.8m long, 1.2m wide and 0.35m deep. The valley slope of the flume S_0 was adjustable with a jack and hinge and was set at 0.001. The main channels and the flood plains were formed of polystyrene boards whose thickness was 53mm and specific gravity was 0.020-0.070. The channel meanders were expressed as combinations of arcs with its central radius r_c of 0.425m and straight reaches with its length L_{co} of 0.374m. The arc of meander φ was changed in order to obtain desired channel sinuosity *s*. The tested *s* were 1.09, 1.37 and 1.57 corresponding φ of 60°, 120° and 180° respectively. The rectangular main channel has its width b and depth h of 0.15m and 0.053m respectively. The other relevant parameters for compound meandering channels are illustrated in Fig. 1. Dimensions of these parameters for the tested channels are summarised in Table 1. A series of meanders with these dimensions was designed in the flume (see Fig. 2).

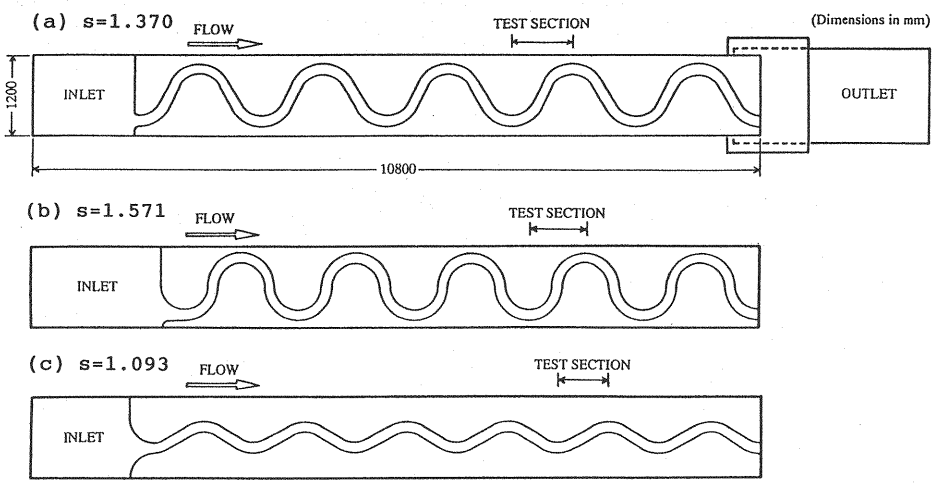

Fig. 2 The experimental flume and meandering channels

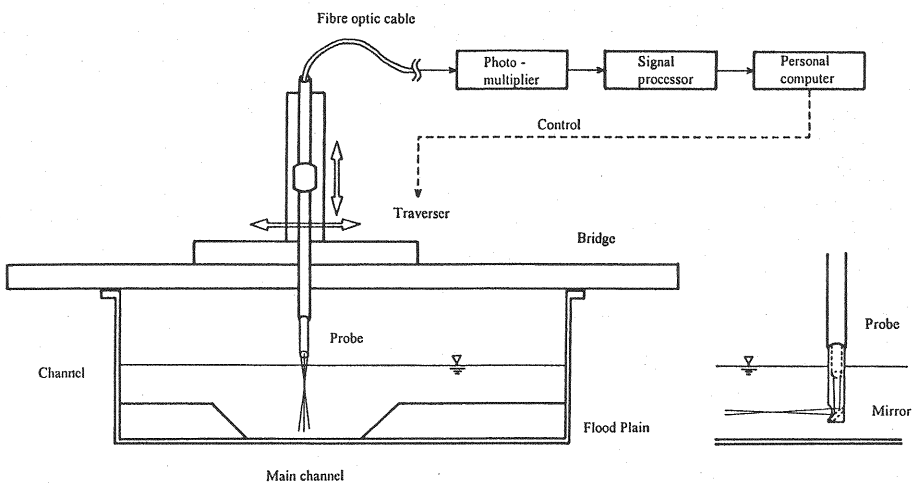

Fig. 3 The laser Doppler anemometry system

A TSI 2 component fibre optic laser Doppler anemometer system was employed for velocity and turbulence measurements. Fig. 3 shows the laser beam installation method together with the signal processing procedure. As can be seen in the figure, measurements for each point were made at least twice with different beam installation methods so that three components of velocity were obtained. The effect of water surface fluctuation for the streamwise (x) and lateral (y) measurements was checked in preliminary experiments and were confirmed to be negligible. It was also verified that the submerged probe for the vertical (z) measurements does not significantly affect the measurement volume. The measurements were carried out using aluminium powder of 28μm mean diameter as a seeding agent. The averaged data sampling rate was about 100Hz. The measuring duration for one point was 60sec.

A half wavelength of the meander channel was devided into 9 to 13 sections and the measurements were performed at every other section (see Fig. 4). The tested hydraulic conditions are summarised in Table 2. Three typical depth conditions were selected for all channels. i.e. the

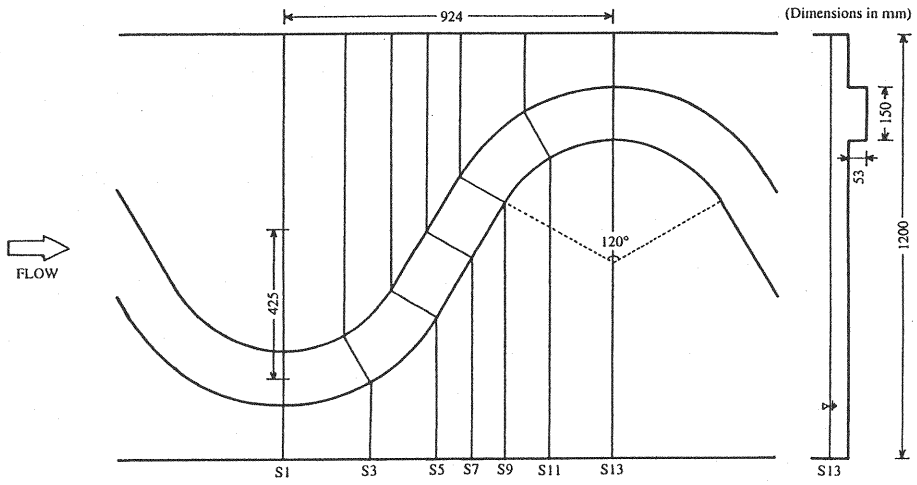

Fig. 4 Tested sections for velocity measurements (s=1.370)

Table 2 Hydraulic conditions

	Depth condition Dr	Discharge Q ($\times 10^{-3} m^3/s$)	Water depth H (m)	Mean velocity U_S (m/s)	Friction velocity u_* (m/s)	Reynolds number Re ($\times 10^4$)	Froude number Fr
R1	bankfull	1.876	0.0525	0.237	0.0166	2.63	0.431
	0.15	3.102	0.0633	0.157	0.0121	0.82	0.412
	0.50	25.755	0.1078	0.352	0.0225	6.26	0.495
R2	bankfull	1.556	0.0519	0.197	0.0148	2.19	0.359
	0.15	2.513	0.0630	0.129	0.0120	0.66	0.340
	0.50	19.996	0.1059	0.282	0.0221	4.92	0.401
R3	bankfull	1.382	0.0532	0.170	0.0140	1.95	0.307
	0.15	2.204	0.0631	0.113	0.0120	0.62	0.299
	0.50	19.881	0.1087	0.268	0.0226	5.16	0.374

bankfull flow and Dr(=(H-h)/H, where H = water depth at the main channel and h = the height of the flood plain)=0.15 and 0.50.

RESULTS AND DISCUSSIONS

Flow in compound meandering channels for overbank flow is extraordinarily complicated since it is brought not only by the velocity difference between the main channel and the flood plain, as is the case for straight compound flows, but by differences of the main stream directions in these sections. Kiely (6), based on the velocity distributions in the main stream direction in each section, pointed out some key structures which he postulated as being essential in compound meandering flows. Here the flow structure in compound meandering channels identified by the detailed velocity and turbulence measurements (Muto (9)) is discussed compared with Kiely's results.

Secondary Flow Structure

Fig. 5 shows secondary flow behaviour from the upstream in a vector form for the bankfull and Dr=0.15 flows in the s=1.37 channel. Fig. 5(a), for the bankfull flow, shows that the dominant secondary flow cell near the inner wall is developed through a bend section, gradually extending its size towards the outer wall. This clockwise cell is fully developed at the bend exit (Section 5), which occupies two-thirds of the whole cross

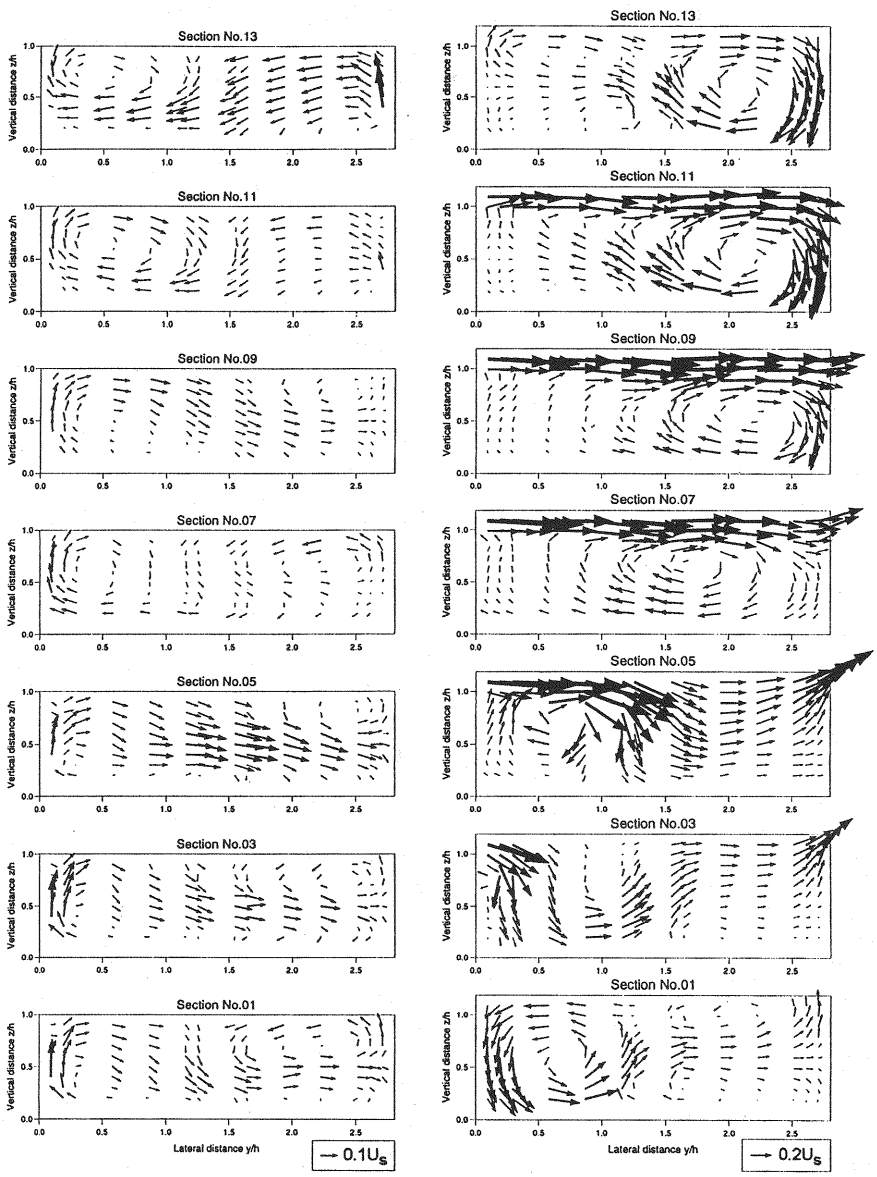

(a) Bankfull (b) Dr=0.15

Fig. 5 Secondary flow vectors in the s=1.370 channel

section. This cell decays gradually along the straight crossover region and the consecutive bend. On the other hand, for the overbank flow, Fig. 5(b), the anticlockwise dominant cell can be recognised at Section 1 as being situated in the vicinity of the inner wall. The cell suddenly collapses in the latter half of the bend synchronous with the appearance of a new clockwise cell along the inner wall from Section 3. This new cell immediately grows and occupies most of the cross section in the crossover region. These results come from the difference of the originating and developing processes of the cell. That is, it is the centrifugal force that governs the flow structure in the inbank case. Whereas for the overbank flow the structure is controlled by the flow

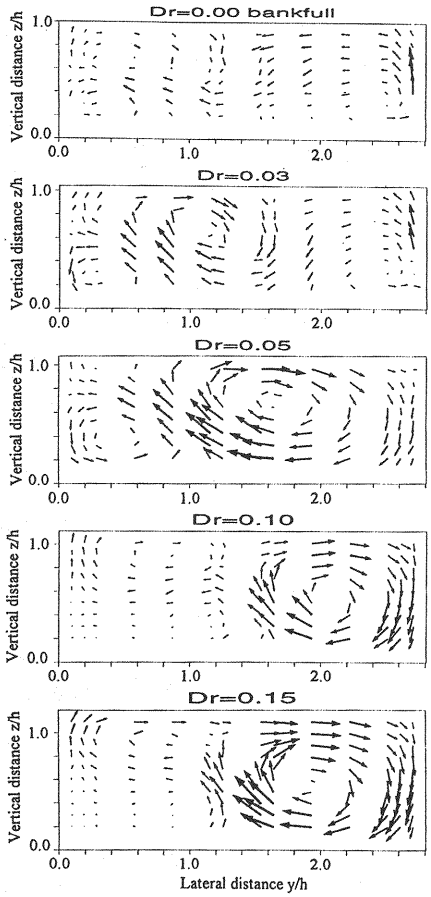

Fig. 6 Secondary flow at a bend apex in various depths (s=1.571)

interaction in the crossover region. This shear layer effect is so strong as to nullify the centrifugal effect in overbank cases. It can be said from these results that the secondary flow structures are different between inbank and overbank flows. The most remarkable is that the rotating directions of cells along the inner wall in a bend are opposite to each other. This is apparently brought by the difference of secondary flow structures described above.

Another series of measurements was conducted in order to identify the critical depth condition for the transition of the secondary flow rotation at a bend apex Section 13 in the s=1.57 channel. The results of secondary flow vectors are shown in Fig. 6. The figure indicates that a clockwise cell starts to develop immediately after inundation and moves towards the inner bank as the flooding depth increases, then it remains there when the depth is greater than Dr=0.10. At Dr=0.03, a curvature-induced anticlockwise cell can still be observed near the inner bank however it disappears at Dr=0.05, which means that shear layer effect overcomes the curvature effect at around that depth condition. Thus it can be concluded that the transition of the dominant mechanism for secondary flow production from the centrifugal force effect (inbank) to the shear layer interaction effect (overbank) takes place at around Dr=0.05.

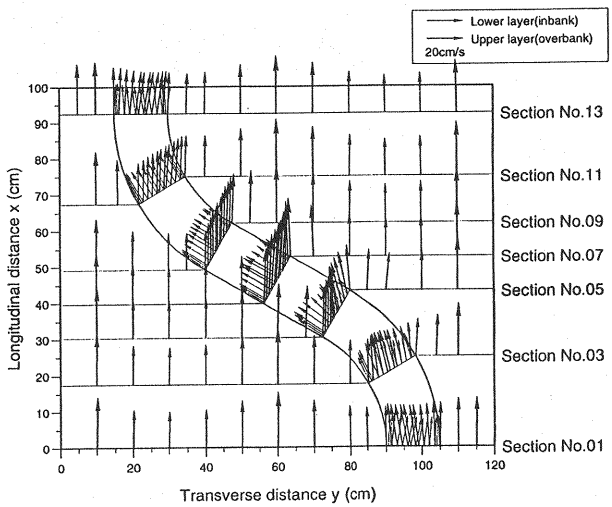

Fig. 7 Layer averaged velocity distribution (s=1.370, Dr=0.50)

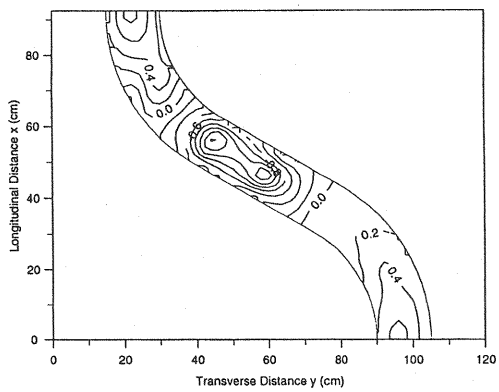

Fig. 8 Reynolds stress $-\overline{uw}/u_*^2$ at the interface (s=1.370, Dr=0.50)

Interaction Process

Interaction between the main channel flow and the flood plain flow, especially that in the crossover region, is one of the key elements in compound meandering channels. Figs. 7 and 8 show the layer averaged velocity distribution and the shear stress distribution at the bankfull level respectively, for Dr=0.50 in the s=1.37 channel. These figures clearly show that large shear stresses are produced in the crossover region because there exist large velocity differences between the upper and lower layer flows both in magnitude and direction.

Fig. 9 shows the vertical distributions of shear stress $-\overline{uw}$ at Section 9 for Dr=0.50, s=1.37 channel. Here the bed shear stress data measured by a Preston tube is used as the bed boundary condition. It can firstly be noticed that the negative peak of the interfacial shear stress at the boundary of the upper and lower layers can reach 2 to 5 times larger in magnitude than the bed shear stress. Secondly the distributions have a strong non-linear nature. Especially in the upper layer, the value suddenly changes from 0 to the peak when approaching the interfacial boundary. It is clear that the traditional linear expression for $-\overline{uw}$

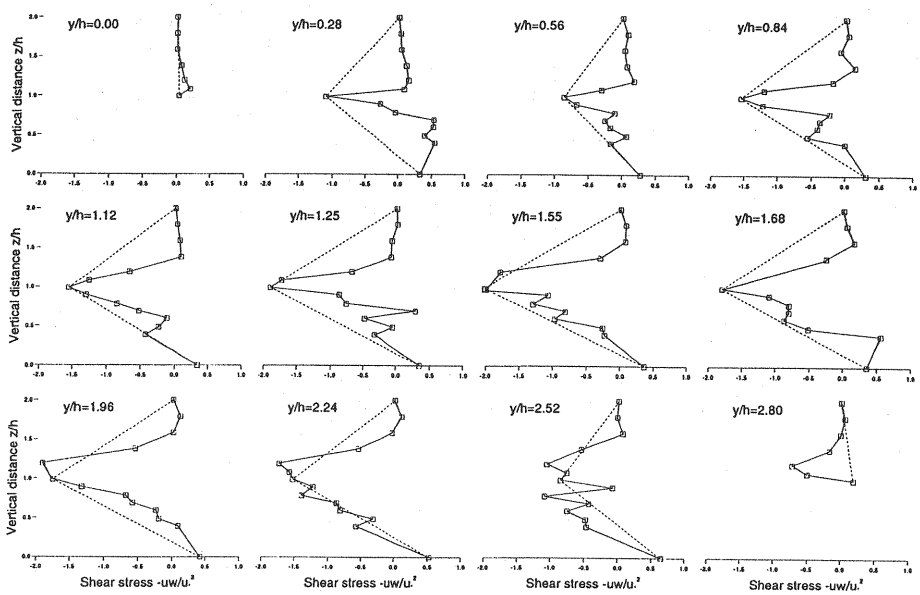

Fig. 9 Vertical distributions of $-\overline{uw}/u_*^2$ in a crossover section (Section 9, s=1.370, Dr=0.50)

distribution cannot be applied to compound meandering flows. Thus a two layer model was considered based on the concept suggested by Knight & Shiono (7). Their concept is the vertically integrated form of the momentum equation:

$$-\rho\overline{uw} = \tau_b - \rho g z S_0 + \int_0^z \left\{\frac{\partial(-\rho\overline{uv})}{\partial y}\right\}dz - \int_0^z \frac{V\partial U}{\partial y}dz - \int_0^z \frac{W\partial U}{\partial z}dz \qquad (1)$$

When applying this to compound meandering flows, it should be taken into account that the flow behaviour suddenly changes at around the bankfull level. In other words, it is thought that fluids which possess different velocities meet each other at that level. In such a case one may assume that the interface works as a loose boundary for the flows on both sides, i.e. the upper and lower layer flows. This will support the concept of dividing the channel into two parts at the bankfull level. Consequently, if the effect of neither secondary flow nor the lateral turbulence exists, the vertical distributions of $-\overline{uw}$ can only be determined by the stresses at the boundaries, i.e. the surface, bed and interface, and are linear in each layer. The broken lines in Fig. 9 are drawn applying this assumptions. In the lower layer, although rather scattered, the distributions more or less follow the linear assumption. Whereas this approximation cannot be applied to the upper layer. The model clearly shows how the secondary flow and turbulence affect the distribution of $-\overline{uw}$.

Fluid Exchange

Willetts & Hardwick (17) conducted flow visualisation in a compound meandering channel and pointed out that fluid running along the outer bend of the main channel emerges onto the adjacent flood plain in the crossover region, simultaneously the flow from the upstream flood plain

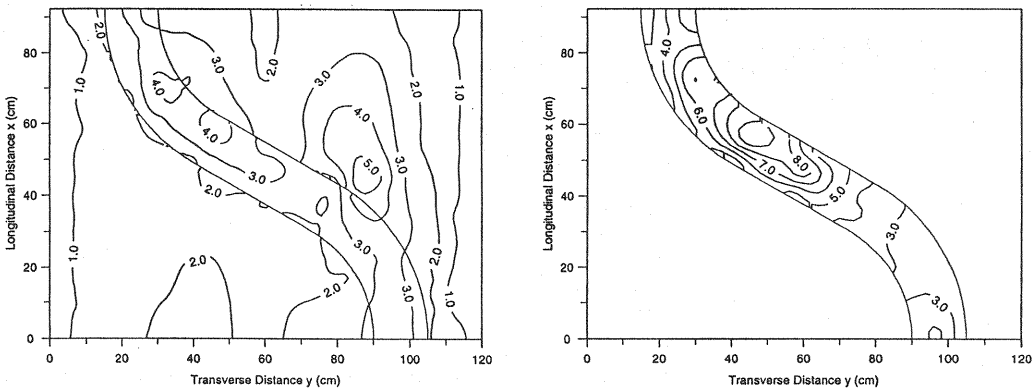

(a) Upper layer (b) Lower layer

Fig. 10 Layer averaged turbulent kinetic energy $\overline{k} / u_*^2$ (s=1.370, Dr=0.50)

is partially entrained in the main channel as if compensating the emerging volume. This mechanism can also be recognised in Figs. 5 and 7.

Layer averaged turbulent kinetic energy $\overline{k}$, where $k=(u'^2+v'^2+w'^2)/2$, for Dr=0.50, s=1.37 channel is shown in Fig. 10. An area producing high turbulent energy is easily recognised on the downstream flood plain next to the bend exit in the upperlayer, whereas such an area is seen from the crossover region to the entrance of the bend in the lower layer. These are good references for the fluid exchange described above. Thus it is deemed that the fluid exchange produces quite large turbulent kinetic energy and therefore largely affects the energy loss mechanisms in compound meandering channels.

CONCLUSIONS

The main results can be summarised as follows:

1) Based on the detailed velocity measurements in compound meandering channels, essential flow structures of secondary flow, flow interaction and fluid exchange are identified, which may largely affect the channel conveyance capacity.
2) For inbank cases it is the centrifugal force that governs the structure of secondary flow. Whereas for overbank cases the structure is controlled by the flow interaction between the lower and upper layers in the crossover region. Consequently the secondary flow structures, including their originating mechanisms, are different between inbank and overbank flows. The transition of the structure from the inbank to the overbank takes place at around Dr=0.05.
3) Interaction between the main channel flow and the flood plain flow produces large shear stress at the bankfull level, especially in the crossover region where the lower and upper layer flows meet in a rather complex way. A 2 layer model is considered to predict vertical distributions of $-\overline{uw}$ and it supports the usefullness of the division method at the bankfull level in compound meandering channels.
4) Layer averaged turbulent kinetic energy shows clear evidence of the fluid exchange between the main channel and the flood plain.
5) These unique structures identified here should be taken into account when considering physical and numerical methods for estimating the high stage during floods in such channels.

ACKNOWLEDGEMENT

The authors gratefully acknowledge the financial support of the Engineering & Physical Sciences Research Council (EPSRC, formerly SERC): Grant No. GR/H14655.

REFERENCES

1. Ackers, P. : Flow formulae for straight two-stage channels, J. Hydr. Res., Vol.31, No.4, pp.509-531, 1993.
2. Ervine, D.A., B.B. Willetts, R.H.J. Sellin and M. Lorena : Factors affecting conveyance in meandering compound flows, J. Hydr. Eng., Vol.119, No.12, pp.1383-1399, 1993.
3. Fujita, M. : Problems of compound channel flows, Lecture Notes of the 25th Summer Seminar on Hydraulics, JSCE, pp.A-9-1 - A-9-17, 1989. (in Japanese)
4. Ishigaki, T. : Three Dimensional Structure of Turbulent Flow in Compound Open Channel, Ph. D. Thesis, Kyoto University, Japan, 1993. (in Japanese)
5. James, C.S. and J.B. Wark : Conveyance Estimation for Meandering Channels, Report SR 329, HR Wallingford, UK, 1992.
6. Kiely, G. : Overbank flow in meandering compound channels. The important mechanisms, Int. Conf. on River Flood Hydraulics, Wallingford, UK, pp.207-217, 1990.
7. Knight, D.W. and K. Shiono : Turbulence measurement in a shear region of a compound channel, J. Hydr. Res., Vol.28, No.2, pp.175-196, 1990.
8. Knight, D.W. and K. Shiono : River channel and floodplain hydraulics, Floodplain Processes, M.G. Anderson, D.E. Walling and P.D. Bates, ed., John Wiley & Sons Ltd., UK, pp.139-181, 1996
9. Muto, Y. : Turbulent Flow in Two-Stage Meandering Channels, Ph. D. Thesis, Bradford University, UK, 1997.
10. Naot, D., I. Nezu and H. Nakagawa : Hydrodynamic behavior of compound rectangular open channels, J. Hydr. Eng., Vol.119, No.3, pp.390-408, 1993.
11. Sellin, R.H.J., D.A. Ervine and B.B. Willetts : Behaviour of meandering two-stage channels, Proc. ICE Wat., Marit. and Energy, Vol.101, pp.99-111, 1993.
12. Shiono, K. and D.W. Knight : Turbulent open-channel flows with variable depth across the channel, J. Fluid Mech., Vol.222, pp.617-646, 1991.
13. Shiono, K. and Y. Muto : Secondary flow structure for in-bank and over-bank flows in trapezoidal meandering channel, Proc. Of the 5th Inter'l Symp. on Refined Flow Modelling and Turbulence Measurements, Paris, France, pp.635-652, 1993.
14. Shiono, K., Y. Muto, J. Alromaih, H. Imamoto and T. Ishigaki : Flow discharge characteristics for overbank flow in meander channel, Proc. of the Inter'l Conf. on Hydro-Science & Engineering, Washington DC, USA, Invited paper, pp.1309-1316, 1993.
15. Shiono, K., Y. Muto, H. Imamoto and T. Ishigaki : Flow structure in meandering channels, Proc. of MAFF Conf., Loughborough University, pp.9.3.15-9.3.26, 1994.
16. Tominaga, A. and I. Nezu : Turbulent structure in compound open-channel flows, J. Hydr. Eng., Vol.117, No.1, pp.21-41, 1991.
17. Willetts, B.B. and R.I. Hardwick : Stage dependency for overbank flow in meandering channels, Proc. ICE Wat., Marit. and Energy, Vol.101, pp.45-54, 1993.

APPENDIX - NOTATION

The following symbols are used in this paper:

- A = Sectional area;
- b = Main channel width;
- B = Total channel width;
- B_W = Meander wave width;
- Dr = Relative depth (=(H-h)/H);
- Fr = Froude number;
- g = Gravity acceleration;
- h = Height of the flood plain;
- H = Water depth at the main channel;
- k = Turbulent kinetic energy ($=\frac{1}{2}(u'^2+v'^2+w'^2)$);
- $\bar{k}$ = Depth/layer averaged turbulent kinetic energy;
- L = Channel length;
- L_{co} = Crossover length;
- L_W = Meander wavelength;
- P = Wetted perimeter;
- Q = Discharge;
- r_C = Central radius of the bend;
- R = Hydraulic radius (=A/P);
- Re = Reynolds number;
- s = Sinuosity;
- S_0 = Channel slope (= sin ø);
- u = Instantaneous streamwise velocity fluctuation;
- u' = Streamwise turbulent intensity (r.m.s. value);
- u_* = Friction velocity ($=\sqrt{gRS}$);
- U_s = Sectional averaged velocity (= Q/A);
- v = Instantaneous lateral velocity fluctuation;
- v' = Lateral turbulent intensity (r.m.s. value);
- w = Instantaneous vertical velocity fluctuation;
- w' = Vertical turbulent intensity (r.m.s. value);
- x = Streamwise distance;
- y = Lateral/Spanwise distance;
- z = Vertical distance;
- θ = Central angle of bend curvature / Angle of crossover;

ρ = Density of water;

τ = A general shear stress;

τ_b = Bed shear stress;

φ = Angle of arc; and

ϕ = Channel gradient ($S_0 = \sin \phi$).

(Received March 4, 1997; revised March 2, 1998)